

VISCOUS WAVE INTERACTION WITH STRUCTURES

Deborah Greaves Department of Architecture and Civil Engineering, University of Bath,
Claverton Down, Bath BA2 7AY U.K. e-mail: d.m.greaves@bath.ac.uk

Many applications of wave interaction with a floating structure can be suitably approximated using potential flow theory, which assumes that the fluid is incompressible and inviscid. However, in some situations, such as the response of a floating wave energy device, flow separation, turbulence and wave breaking all make significant contributions to the fluid loading. In these cases, the fluid viscosity must be accounted for, which usually means solving the full Navier-Stokes equations or RANS equations if the flow is turbulent. To model wave breaking a two-fluid approach may be taken, in which the fluid flow equations are solved both in air and water so that complex free surface motions can be modelled including wave overturning and break up into spray.

This work involves the application of adaptive hierarchical grids to free surface Navier-Stokes simulation of viscous waves over a submerged cylinder in a stationary tank. Adapting quadtree grids (Greaves and Borthwick, 1998) are combined with a volume of fluid (VoF) approach, in which the CICSAM high resolution interface capturing scheme, derived by Ubbink (1997), is used for advection of the interface. The Navier-Stokes equations are discretised using finite volumes with collocated primitive variables and solved using Issa's (1986) PISO (Pressure Implicit with Splitting of Operators) algorithm. The cylinder is included by using the technique of Cartesian cut cells described by Causon *et al.* (2000).

Waves in viscous fluid

The new method is used to simulate small amplitude viscous waves in a unit square tank, for which Wu *et al.* (2001) describe the linear analytical solution. In Wu *et al.*'s (2001) solution, no shear conditions are used on the tank walls, which is equivalent to the slip boundary conditions used in the numerical solution. The liquid is given an initial cosine wave elevation, $h = a \cos(2\pi x/b)$, where x is measured along the length of the tank, b is the length of the tank and $a = 0.01$ is the wave amplitude. Here, grid adaptation is used to follow the movement of the free surface and refinement is provided in a band surrounding the air-water interface. Remeshing of the grid operates by dividing a cell into four if it lies on the free surface; derefinement takes place by removing four sibling cells and replacing them with their parent if each of the four sibling cells lies away from the free surface.

For the first case considered, the Reynolds number, $Re = d\sqrt{gd}/\nu = 200$, where d is the mean water depth. Results are presented by plotting the free surface elevation, $h = y/a$, recorded at the centre of the tank against non-dimensional time, $t = t\sqrt{g/d}$. In Figure 1, results of calculations on quadtree grids of different resolution are plotted, and in Figure 2, results of different time step size are summarised for the 7×5 quadtree grid. These demonstrate spatial and temporal grid convergence of the method. In Figures 3 - 6, time history results are plotted for waves in fluid of different viscosity, $Re = 2, 20, 200$ and 2000 , together with the analytical

solution published by Wu *et al.* (2001). In each case, the wave period is generally predicted well by the numerical scheme, but the wave amplitude is greater than the linearised analytical solution. The numerical prediction is closer to the linearised analytical solution for larger Reynolds number (less viscous fluid).

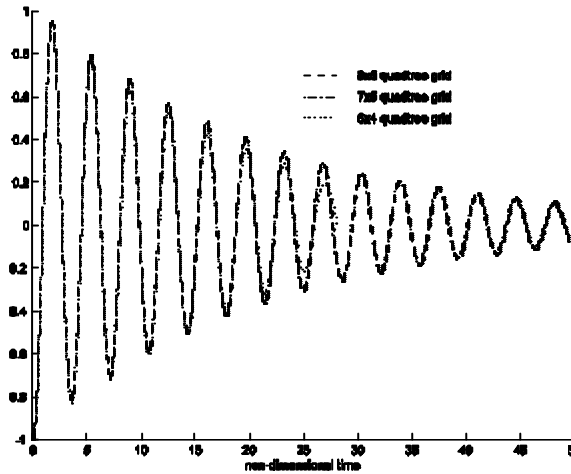


Figure 1 Comparison of quadtree grid sizes

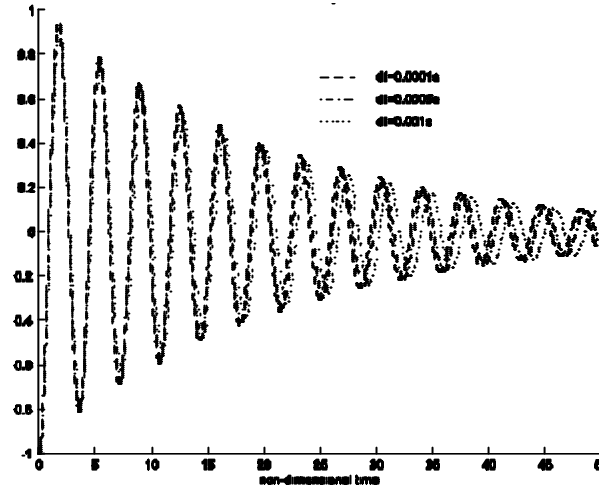


Figure 2 Comparison of time step

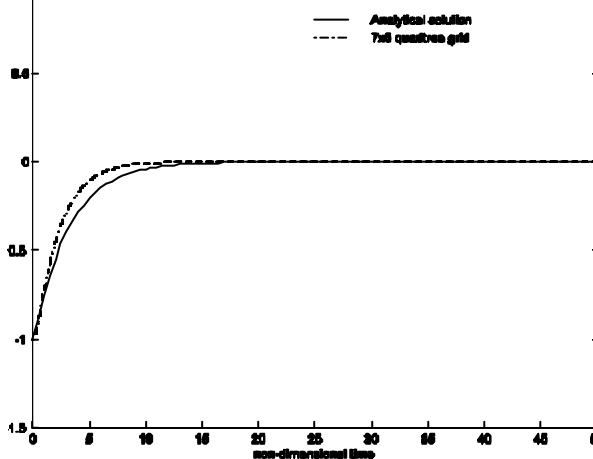


Figure 3 $Re = 2$

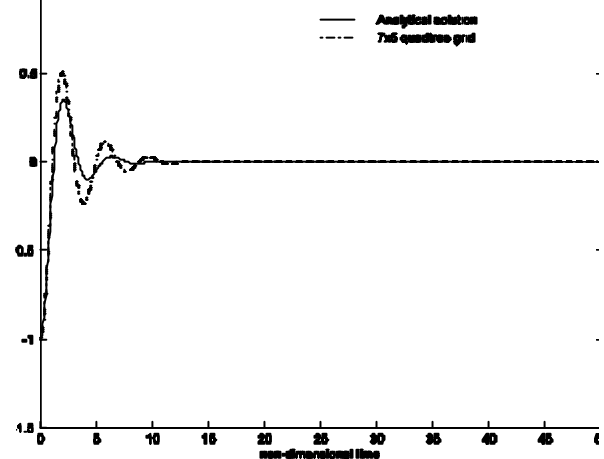


Figure 4 $Re = 20$

Separated flow past a cylinder

Quadtree grids may be used to model boundaries of arbitrary shape. However, due to their Cartesian nature, smooth curves will have a stepped approximation. This modelling error can be eliminated by using the Cartesian cut cell technique, in which the smooth shape of the body is cut out of the grid, leaving cut cells around the body boundary. Special interpolations are used to calculate gradients and variables at faces for the finite volume scheme at these cut cells. The adaptive quadtree cut cell method is first tested for fluid flow past a cylinder at Reynolds number, $Re = 100$. The grid is initially refined around the cylinder boundary only, and as the vortex shedding flow develops, it adapts to areas of high vorticity. Figure 7 shows the velocity vectors once vortex shedding has established at non-dimensional time, $T=tD/u_{in}$

= 129 (where D is the cylinder diameter and u_{in} is the inlet velocity). Figure 8 shows the time history of lift and drag force coefficients. The Strouhal number is predicted to be 0.143, the mean drag coefficient to be 1.39 and the rms lift coefficient to be 0.13, which agree reasonably with experimental and numerical data given by Zhou and Graham (2000).

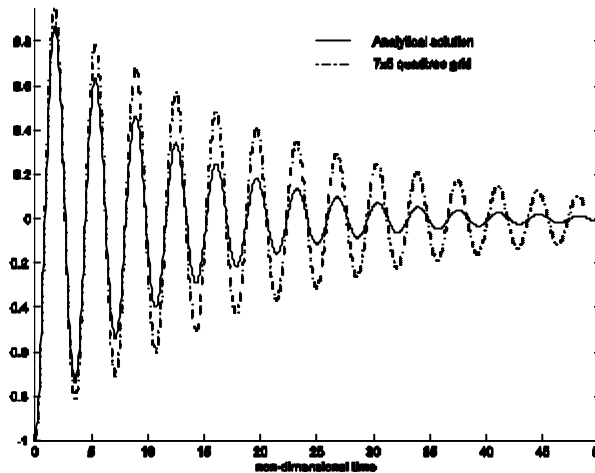


Figure 5 $Re = 200$

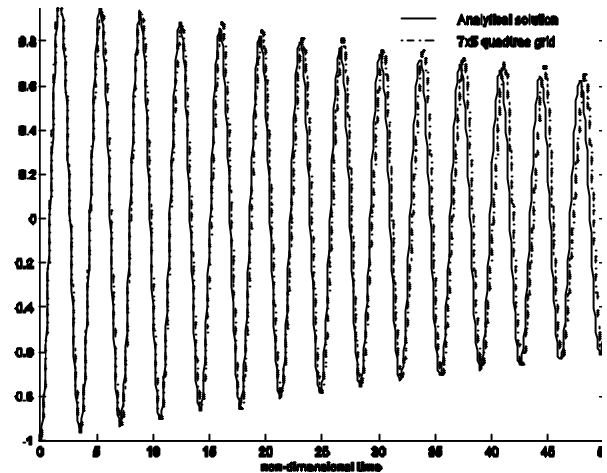


Figure 6 $Re = 2000$

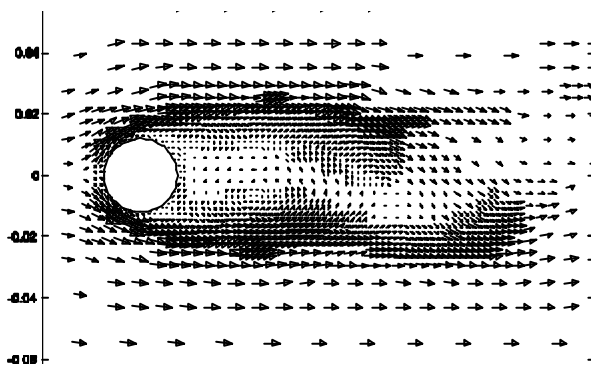


Figure 7 $T = 129$ velocity vectors

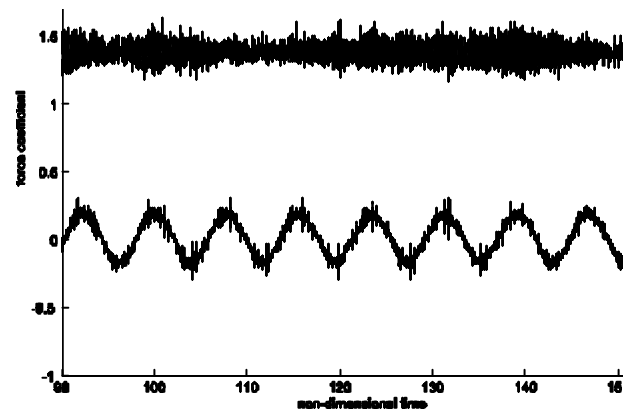


Figure 8 Time history of c_D and c_L for $Re = 100$

Waves in viscous fluid over a submerged cylinder

In this case, a submerged cylinder of diameter 0.1 is positioned at the horizontal centre of the unit square tank at depth 0.25 below the mean water level. The lower fluid Reynolds number, $Re = d\sqrt{gd}/\mathbf{n} = 200$. A refinement band of 10 cells is maintained around the interface and the grid adapts dynamically at each time step. The initial grid is shown in Figure 9 and the time history of the wave recorded at the centre of the tank is plotted in Figure 10 together with the wave-only case without a cylinder for comparison. Calculations are made both on adapting quadtree grids and a fixed uniform grid of the smallest cell size (128 x 128). Preliminary results from both grids are plotted in Figure 10 and the difference between the

two negligible. The results show that the presence of the submerged cylinder in the tank acts to damp out the wave motion at the free surface. Use of adapting quadtree grids is found to achieve the same accuracy, but reduce both the computer storage and CPU cost when compared with equivalent uniform grid calculations.

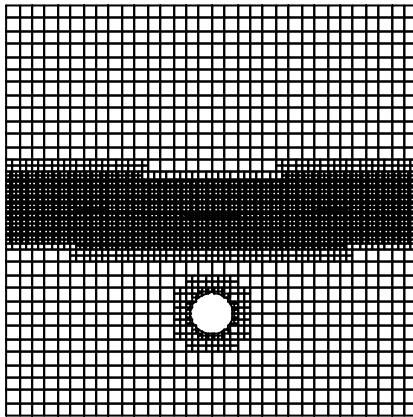


Figure 9 Initial grid

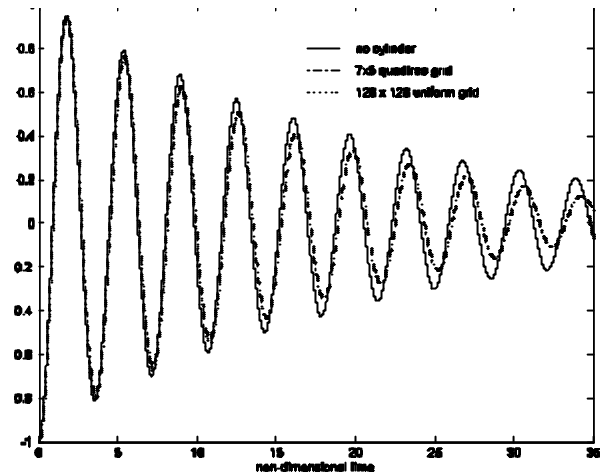


Figure 10 Wave elevation time history, $Re=200$

The author is very grateful to the Royal Society for supporting this work through a Royal Society University Research Fellowship.

References

- Causon, D.M., 2000 Calculation of shallow water flows using a Cartesian cut cell approach, *Advances in Water Resources*, **23**(5), 545-562.
- Greaves, D.M. and Borthwick, A.G.L. 1998 On the use of adaptive hierarchical meshes for numerical simulation of separated flows, *International Journal for Numerical Methods in Fluids*, **26**, 303-322, ISSN 0271-2091.
- Issa, R.I. 1986 Solution of the implicitly discretised fluid flow equations by operator-splitting. *J. Computational Physics*, **62**(1), 40-65.
- Monnier, J. and Witomski, P. 2004 A Hydrodynamic model with local Marangoni effects arising from microfluidics, *Proc. 4th European Congress on Computational Methods in Applied Sciences and Engineering*, July 24-28 2004 Jyväskylä, Finland.
- Ubbink, O. 1997 *Numerical prediction of two fluid systems with sharp interfaces*, PhD Thesis, Imperial College of Science, Technology and Medicine, London.
- Wu, G.X., Eatock Taylor, R. and Greaves, D.M. 2001 Viscous effect on the transient free surface flow in a two dimensional tank, *Journal of Engineering Mathematics*, 2001; vol. 40, 77-90, ISSN 0022-0833.
- Zhou, C.Y. and Graham., M.R. 2000 A numerical study of cylinders in waves and currents, *Journal of Fluids and Structures*, **14**, 403-428.